A single-crystal silicon micromirror for large bi-directional 2D scanning applications

Ankur Jain *, Huikai Xie

Department of Electrical and Computer Engineering, University of Florida, Gainesville, USA

Abstract

This paper reports the design, fabrication and operation of a two-dimensional (2D) micromirror that can generate large bi-directional scans at low actuation voltages. This single-crystal silicon (SCS) micromirror device has been fabricated by using a unique DRIE CMOS-MEMS process that can simultaneously provide thin-film and SCS microstructures. A fabricated micromirror has negligible initial tilt angle, and can perform large bi-directional 2D optical scans (over $\pm 30°$) at less than 12 V dc. 2D dynamic scanning using this mirror has been demonstrated by obtaining a $14° \times 50°$ angular raster scan pattern. This device can also perform vertical displacements up to 0.5 mm at about 15 V dc.
© 2005 Elsevier B.V. All rights reserved.

Keywords: Bi-directional scanning; Electrothermal actuation; Large rotation angle; Large vertical displacement; Optical scanner; Two-dimensional (2D) micromirror

1. Introduction

Micromirrors are widely used for a variety of applications, such as optical displays [1,2], biomedical imaging [3–5], optical switching [6–8], and laser beam steering [9]. However, micromirrors specifically designed for use inside endoscopic probes for internal-organ biomedical-imaging applications must meet requirements of small size, fast scanning speed, large scan angles, and low operating voltage. Numerous two-dimensional (2D) scanning micromirror designs have been developed using electromagnetic, piezoelectric, electrostatic or electrothermal techniques.

2D electromagnetic micromirrors can achieve large rotation angles of $\pm 10°$–$23°$ at low actuation voltages [7,8,10], but they require large external magnets. Therefore, it is challenging to use electromagnetic micromirrors for endoscopic applications which have stringent size restrictions. Piezoelectrically actuated 2D micromirrors have simple structures, but their rotation angles are limited to a few degrees [11–13]. Electrostatically actuated micromirrors can perform fast scanning and consume very low power, but they normally need high driving voltages on the order of 100 V. 2D electrostatic micromirrors using the parallel-plate

electrostatic force have demonstrated rotation angles ranging from $\pm 5°$ up to $\pm 8°$ at driving voltages of 70–200 V [6,14–16]. There is also a trade-off between the mirror-plate size and the maximum allowable rotation angle due to the gap between the electrodes. Other 2D mirror designs used electrostatic comb fingers to achieve larger rotation angles ranging from $\pm 6.2°$ to $+11°$ at actuation voltages between 55 and 140 V [9,17–19]. However, the high voltages required for large angular actuation still remains a deterring factor for their use in certain applications, such as in endoscopes for internal biomedical imaging.

Electrothermally actuated 2D micromirrors with rotation angles of $15°$–$40°$, resonant frequencies in the kHz range, and driving voltages of 15–20 V have been demonstrated [20,21]. Even though electrothermal micromirrors generally consume relatively high power, their large rotation angles with low driving voltages make them ideal for the intended endoscopic bio-imaging applications.

In previous work, we presented single-crystal silicon (SCS) based 1D and 2D micromirrors that used electrothermal actuation to achieve large angular displacements at low driving voltages for endoscopic optical coherence tomographic imaging [3,21]. These mirrors used aluminum/silicon dioxide bimorph beams with an embedded polysilicon heater for electrothermal actuation. However, the unidirectional operation, non-stationary center of rotation, and large initial tilt angle of those micromirrors complicated the device packaging and optical design.

* Corresponding author. Present address: 136 Larsen Hall, P.O. Box 116200, Gainesville, FL 32611-6200, USA. Tel.: +1 352 392 1049; fax: +1 352 846 1416.
E-mail addresses: ajain@ufl.edu (A. Jain), hkxie@ece.ufl.edu (H. Xie).

In this paper, we present a new 2D micromirror device which has a small initial tilt angle and can perform large bi-directional scans at low dc voltages. This new 2D micromirror design uses two sets of large-vertical-displacement (LVD) microactuators [22], to keep the mirror surface parallel to the substrate and also provide bi-directional scanning capability. The device design and fabrication process are reported in Sections 2 and 3. Section 4 describes the micromirror characterization, including the 2D scan patterns.

2. Micromirror design

A schematic view of the 2D micromirror with its nomenclature is illustrated in Fig. 1. The 0.5 mm × 0.5 mm mirror plate is attached to a rigid silicon frame by a set of bimorph aluminum/silicon dioxide thin-film beams. This first set of bimorph beams is referred to as actuator 1 (Act1). As shown in Fig. 1(c), polysilicon resistors embedded in the bimorph beams are used for electrothermal actuation. This frame is connected to a second outer frame by another set of identical bimorph thin-film beams, known as actuator 2 (Act2). After the device is released during fabrication, the bimorph beams curl up due to the tensile stress in the upper aluminum layer and compressive residual stress in the bottom silicon dioxide layer, as illustrated in Fig. 1(c). The rigidity of the frames and the flatness of the mirror are guaranteed by the thick single-crystal silicon layer underneath the frames and mirror. In contrast, the bimorph actuators do not have the SCS layer and thus are thin and compliant in the z-direction. The mirror surface is coated with aluminum for broadband and high reflectivity. The fabrication details are provided in the next section.

Act1 and Act2 together form a large-vertical-displacement microactuator set, in which the curls of the two sets of bimorph beams compensate each other resulting in zero initial tilt of the mirror plate. A detailed analysis on LVD microactuators has been reported in [22,23]. Bi-directional 1D line scanning along the y-axis is possible using this LVD microstructure by alternately applying voltage to actuators Act1 and Act2. In order to enable 2D scanning, a second set of LVD actuators (Act3 and Act4) is attached to the first, as shown in Fig. 1(a). The orthog-
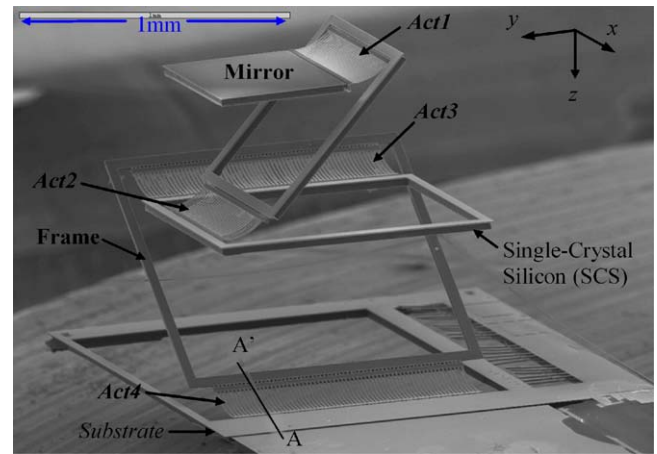

Fig. 2. SEM of a fabricated 2D micromirror. The cross-sectional view of AA′ is shown in Fig. 1(c).

onal orientation of the two sets of LVD actuators results in two perpendicular axes of rotation for the micromirror.

The SEM of a fabricated device is shown in Fig. 2. Each side of the three rectangular frames is 40 μm wide, and has a 40-μm thick SCS layer under it to provide rigidity and thermal conduction to the substrate. The heating element in the bimorph beams is a set of 200-μm long, 7-μm wide polysilicon strips oriented along the beams. As the applied current through the embedded polysilicon resistor increases during actuation, the temperature of the bimorph actuator increases. Since, the top aluminum has a greater thermal coefficient of expansion than the bottom silicon dioxide, the bimorph beams bend downward with increasing temperature, which results in a downward angular displacement of the attached mirror/frame. The primary mirror-rotation directions for actuators 1–4 are along the $+y$, $-y$, $+x$, and $-x$ axes, respectively. However, the heating of the active actuators will cause unwanted rotations by the other actuators due to thermal coupling. This issue is discussed in Section 4.

In order to enable independent electrical excitation for each of the four actuators, a wiring schematic as shown in Fig. 3 is used. The metal-1 aluminum layer on top of the bimorph beams is electrically divided into several paths to carry the different
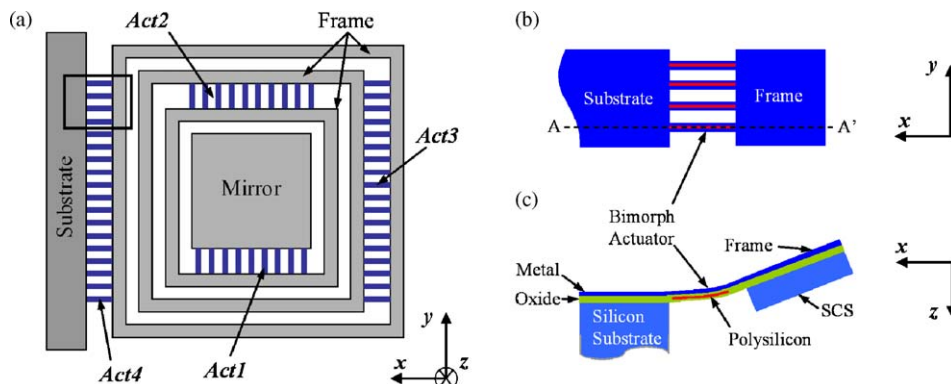

Fig. 1. Micromirror design: (a) top view of the 2D micromirror, highlighting the four bimorph actuators; (b) top view of the actuator area boxed in part (a); (c) cross-sectional view of the bimorph actuator as seen across AA′.
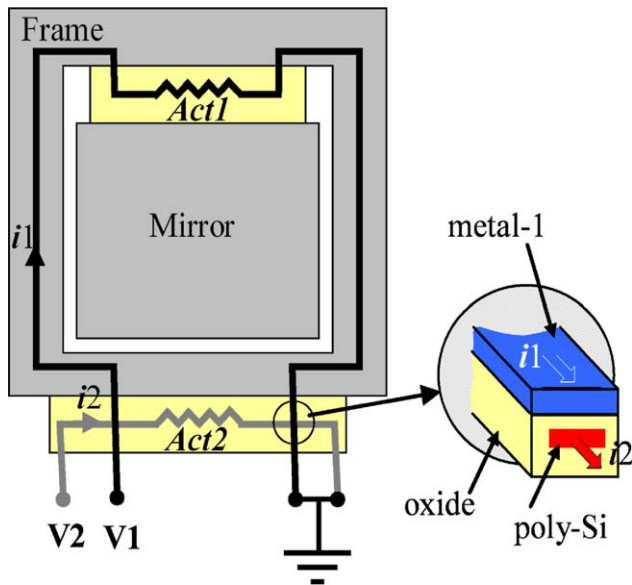
Fig. 3. Layout of the wiring schematic for the LVD actuators. Inset: section of an *Act*2 bimorph beam showing that *Act*1 current is carried by metal-1 layer.

actuation currents for the inner actuators. For example, the metal-1 layer on *Act*4 has been divided into four electrical paths (including the ground line) that carry currents for actuators 1–3. As seen in the inset of Fig. 3, the actuation current which flows though the polysilicon heater is electrically isolated from the current flowing through the metal-1 layer by a thin oxide layer.

3. Device fabrication

The 2D micromirror is fabricated using a deep-reactive-ion-etch (DRIE) CMOS-MEMS process [24]. The post-CMOS process flow, outlined in Fig. 4, uses only four dry etch steps and can simultaneously produce both thin-film and bulk-Si microstructures. The AMI 0.5-μm 3-metal CMOS process available through the MOSIS foundry service [25] was used for the CMOS fabrication.

The CMOS-MEMS process starts with a backside anisotropic silicon etch to form a 40-μm thick SCS membrane (Fig. 4(a)). This SCS membrane is required to keep the mirror flat, and it also provides rigidity to the movable frames. The second step is a frontside anisotropic oxide etch that uses the CMOS interconnect metal (i.e., aluminum) as an etching mask. Next, a deep silicon trench etch is performed to release the microstructure (Fig. 4(c)). The last step is an isotropic silicon etch, performed to undercut the silicon to form bimorph thin-film beams which are about 2 μm thick (Fig. 4(d)). These thin-film beams provide z-axis compliance for out-of-plane actuation, and form bimorph actuators with an embedded polysilicon heater (Fig. 1(c)). There is no substrate or other microstructures directly above or below the mirror microstructure, so large actuation range is allowed. As seen in the SEM of the 2D mirror in Fig. 2, the initial tilt angle of a fabricated mirror plate is less than 0.5°, and its rest position is 1.24 mm above the substrate plane.
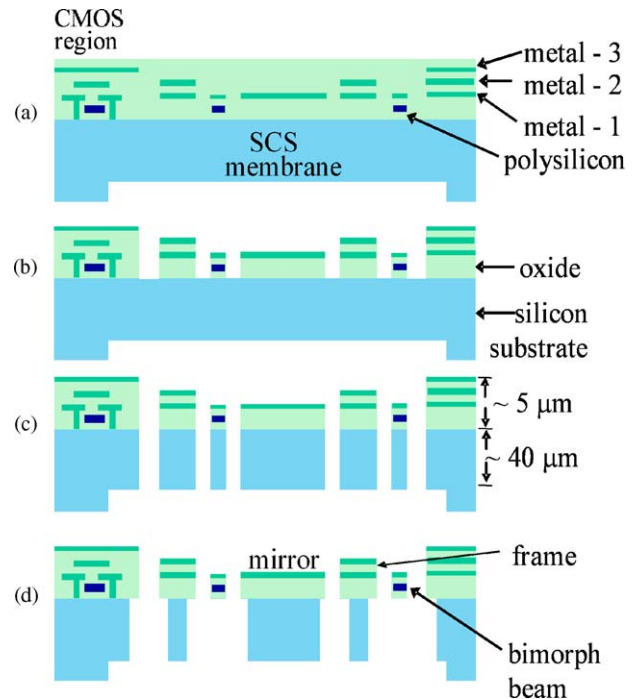

Fig. 4. DRIE CMOS-MEMS process: (a) backside Si etch; (b) oxide etch; (c) deep Si trench etch; (d) Si undercut.

4. Experimental results

4.1. Bi-directional scanning

An experimental setup with a laser beam incident on the mirror and dc voltages applied to the four actuators was used to determine the static 2D scanning response of each actuator. The optical angle scanned by the mirror was determined by measuring the displacement of the reflected laser beam on a calibrated x–y screen. Fig. 5(a) shows the static 2D line scans obtained by actuating each actuator individually, in which only *Act*4 scans along its primary axis while the other scan lines deviate from their primary axes. The corresponding scan-angle versus actuation-voltage characteristics for each of the four actuators are shown in Fig. 5(b). *Act*4 scans along the −x-axis, while *Act*1, *Act*2 and *Act*3 scan 1D lines angled at +60°, −66°, and −28° with respect to the x-axis, respectively. This 2D micromirror device scans optical angles greater than ±40° in the x-direction, and over ±30° in the y-direction at dc actuation voltages less than 12 V. The deviation of a line scan from its primary axis in Fig. 5(a) is caused by thermal coupling between the actuators. Since, *Act*4 is directly connected to the silicon substrate it is least affected by thermal coupling, and this can be observed in Fig. 6(a), where *Act*4 scanned consistently along the −x-direction for different *Act*1 bias voltages. The thermal coupling between the actuators can be modeled by extending the LVD electrothermal model reported in [23,26].

The resistances of the polysilicon heaters embedded in all four actuators increase significantly with applied voltage because of Joule heating. Joule heating raises the temperature of the bimorphs and this increases the heater resistance due to the
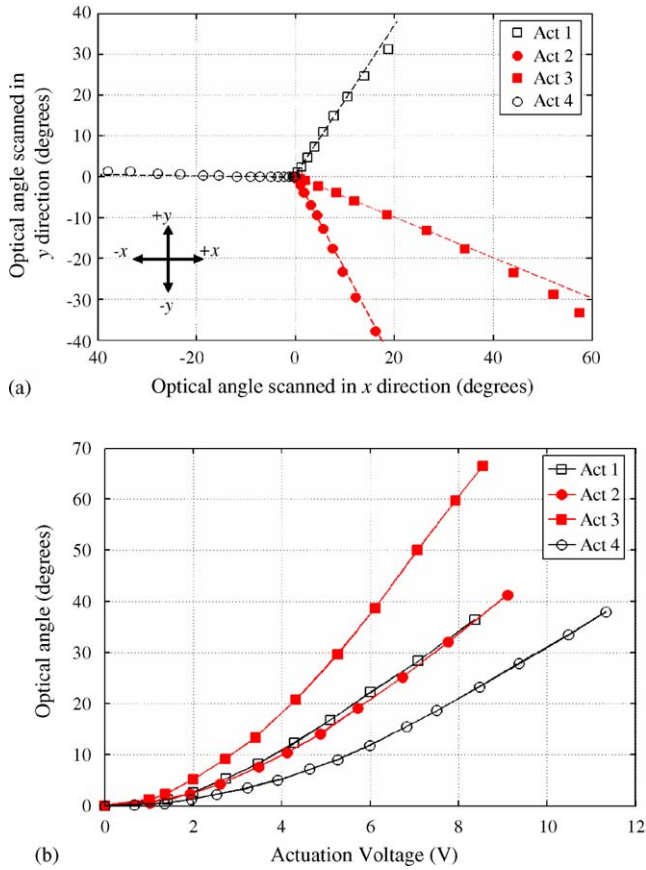
(a)

(b)

Fig. 5. (a) Plot showing the optical angles scanned in 2D space when each actuator is individually actuated. (b) Plot of the effective optical angle scanned vs. actuation voltage for each actuator. *Act*4 scans along −*x*, while *Act*1, *Act*2 and *Act*3 scan at +60°, −66°, −28° with respect to the *x*-axis, respectively.
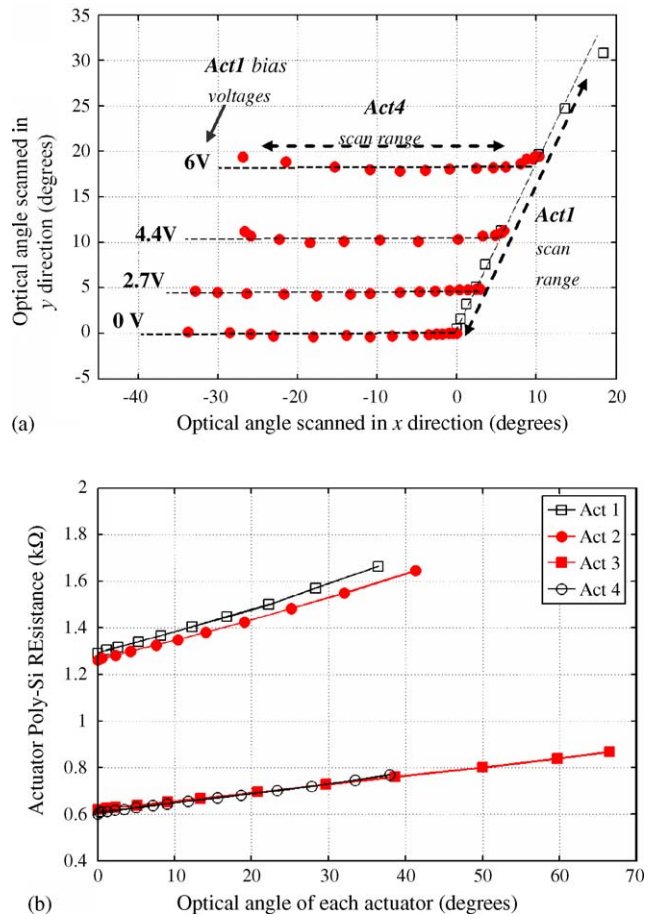

(a)

(b)

Fig. 6. (a) Plot showing the linear scan pattern during static 2D scanning of *Act*1 and *Act*4 only. *Act*4 was actuated at different *Act*1 bias voltages; (b) linear plot of actuator resistance vs. optical scan angle for each actuator.

thermal coefficient of resistivity of polysilicon. The measured polysilicon resistance of each actuator is listed in Table 1. A linear correlation between the optical scan angle and the polysilicon resistance for each of the four actuators was observed, as shown in Fig. 6(b). This correlation allows for independent control of the rotation angle of each actuator by monitoring the resistance of each individual polysilicon heater. Thermal coupling between the actuators can also be accounted for by monitoring the individual polysilicon heater resistances.

The angular stability of the micromirror (at its maximum *xy* tilt angle) was experimentally determined with respect to time, as shown in Fig. 7. From this plot it was determined that the micromirror stability for *Act*1 and *Act*4 were within 0.6° and 0.16°, respectively, for their entire optical scan ranges (which

are 36° and 38°). The initial tilt angle of the mirror plate at different environmental temperatures was also documented, and the results are presented in Fig. 8. For this experiment, the micromirror was heated by a thin-film micro-heater placed under a packaged device, and the tilting of the mirror plate at different temperatures was monitored. Theoretically, a uniform change in
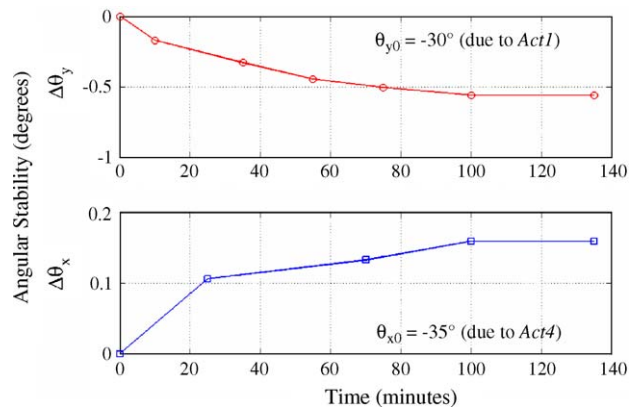
Table 1
Summary of actuator characteristics

Actuator	Heater resistance (kΩ)	Maximum static optical scan angle	Mirror rotation direction	Resonant frequency (Hz)
*Act*1	1.3	36° at 8.4 V	−30° to +*y*-axis	870
*Act*2	1.3	41° at 9.1 V	24° to −*y*-axis	452
*Act*3	0.62	66° at 8.5 V	−28° to +*x*-axis	312
*Act*4	0.62	38° at 11.4 V	along −*x*-axis	170

Fig. 7. Tilt angle stability of the mirror plate vs. time. *Act*1 and *Act*4 were excited to rotate the mirror to its maximum scan angle.
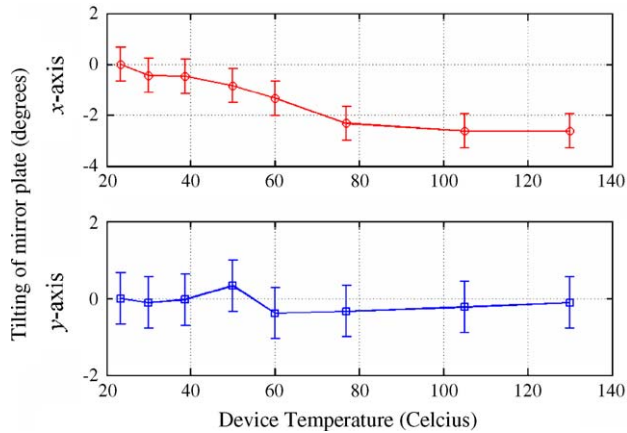
Fig. 8. Initial tilt angle of the mirror plate in x and y directions at different environmental temperatures.

device temperature would cause equal rotational displacements by all four actuators, thereby negating any net mirror tilting. However, as observed in Fig. 8, there is significant mirror tilting in the $-x$-direction and this is attributed to the fact that $Act4$ is heated more than the other actuators since it is directly connected to the substrate, which in turn is directly connected to the heat source.

4.2. Two-dimensional dynamic scanning

2D scanning using this device was demonstrated by simultaneously exciting both $Act1$ and $Act4$ actuators with small ac voltage signals. The frequency and phase of the ac signals were varied in order to generate the Lissajous figures shown in Fig. 9. This device exhibits resonant peaks at 870 Hz, 452 Hz, 312 Hz, and 170 Hz due to the different actuators as summarized in Table 1.

A 2D raster-scanning pattern was generated by the micromirror when $Act1$ was supplied with 1 V dc plus 1 V ac at its resonance of 870 Hz, while $Act4$ was supplied with 2 V dc plus 2 V ac at 15 Hz. As shown in Fig. 10, 58 parallel lines were
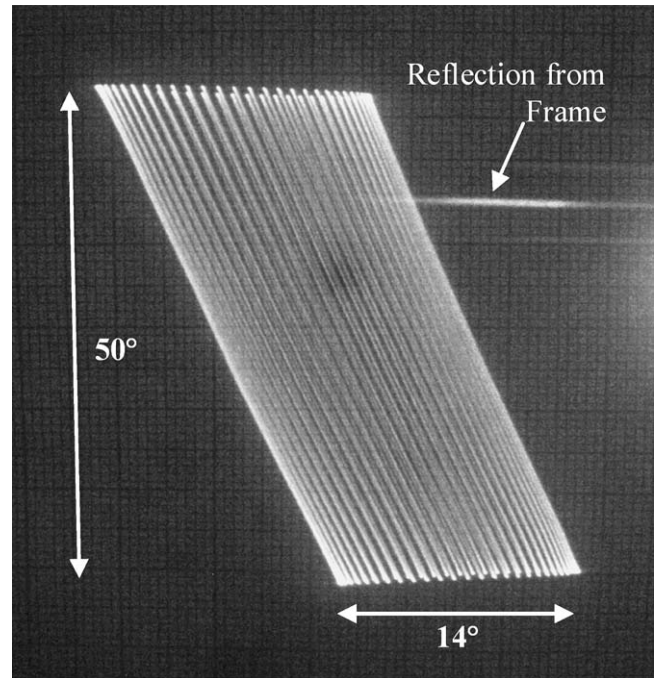

Fig. 10. Resonance scan pattern obtained using actuators 1 and 4.

scanned in a raster-scan pattern by the laser beam covering a $14° \times 50°$ parallelogram angular area.

4.3. Vertical displacement motion

Vertical displacement of the mirror plate can be achieved by equal but opposite angular rotations of only one set of LVD microactuators. For this experiment, only actuators 3 and 4 were used. The $Act3$ actuation voltage was increased in small increments to rotate the mirror plate in the $+x$-direction. This $+x$-direction mirror rotation was compensated by supplying voltage to $Act4$, which rotates the mirror along the $-x$-direction. The opposite rotations brought about by actuators 3 and 4, result in pure vertical displacement of the micromirror along the $+z$-
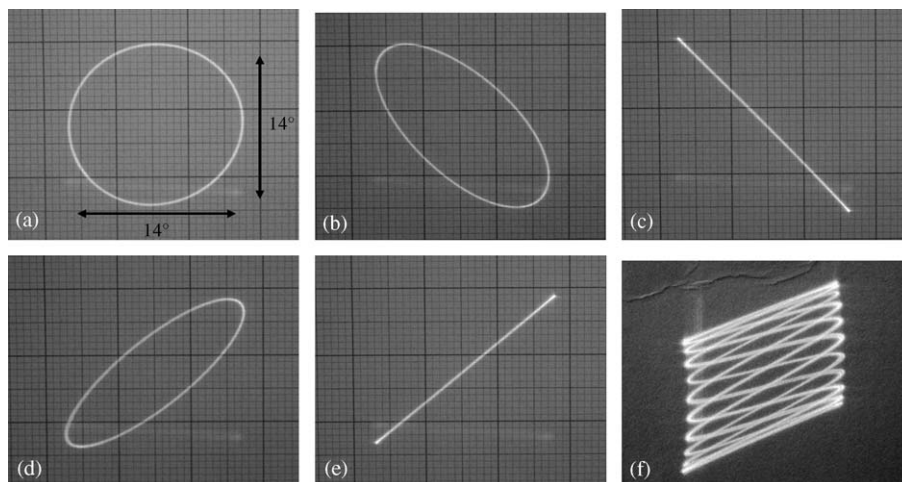

Fig. 9. Photographs of 2D scan patterns: (a)–(e) Lissajous figures scanned by the micromirror by varying only the phase of the excitation signals; (f) Lissajous figure scanned at an excitation frequency ratio of 1:10.
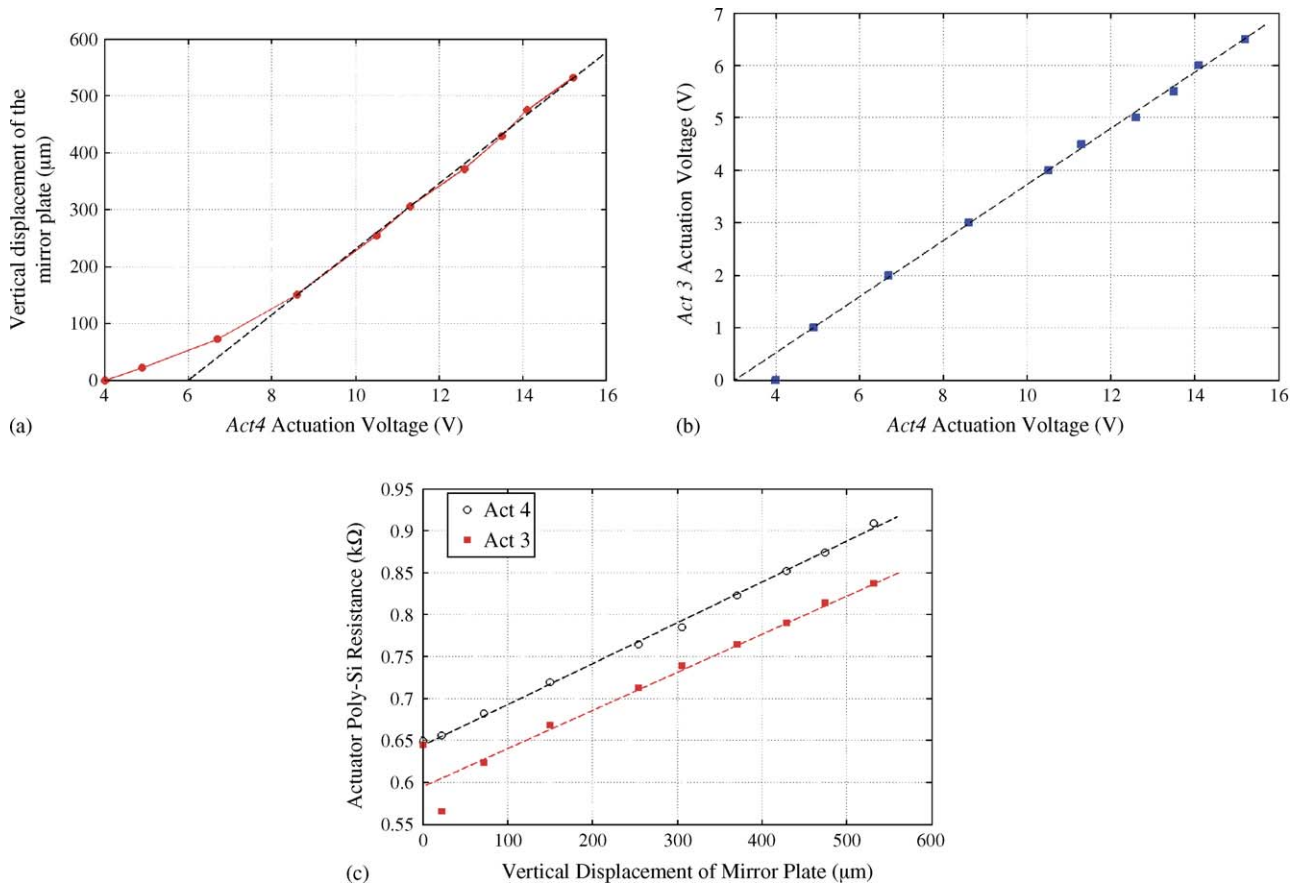
Fig. 11. (a) Vertical displacement of the mirror plate as a function of *Act*4 voltage; (b) corresponding plot of the relationship between *Act*3 and *Act*4 voltages that is required to generate the displacement shown in (a); (c) linear increase of *Act*3 and *Act*4 resistance with vertical displacement.

direction. It should be noted that due to thermal coupling, the inactive actuators 1 and 2 will tilt the mirror plate along the *y*-direction. The vertical displacement of the center of the mirror plate as a function of *Act*4 voltage is shown in Fig. 11(a). It can be seen that a maximum *z*-displacement of 0.53 mm was observed at an *Act*4 voltage of 15 V. Fig. 11(b) shows the almost linear relationship between the *Act*3 voltage and the corresponding *Act*4 voltage that is required to vertically displace the micromirror as obtained in Fig. 11(a). Using this voltage relationship, the *x*-axis tilting of the mirror plate was less than 0.8° during the entire 0.53 mm actuation range. An almost linear correlation between the vertical displacement of the mirror plate and the actuator resistances was observed, as shown in Fig. 11(c). This linear relationship provides a closed-loop feedback path for determining mirror displacement by monitoring the actuator resistances. The *z*-axis vertical scan provided by actuators 3 and 4, in combination with the *y*-axis resonance scan provided by *Act*1 will generate 2D scans in the *y*–*z* plane.

As mentioned above, thermal coupling between the active *Act*3 and *Act*4 actuators causes rotation by *Act*1 and *Act*2 in the orthogonal *y*-direction. This *y*-axis tilting of the mirror plate was monitored and is plotted as a function of vertical displacement in Fig. 12. A maximum *y*-direction mirror-plate tilting of −7° was observed. This −*y* mirror tilting is mainly due to the heating of *Act*2 by the *Act*3 and *Act*4 active actuators. Even with thermal coupling it is possible to scan a 2D depth scan using this
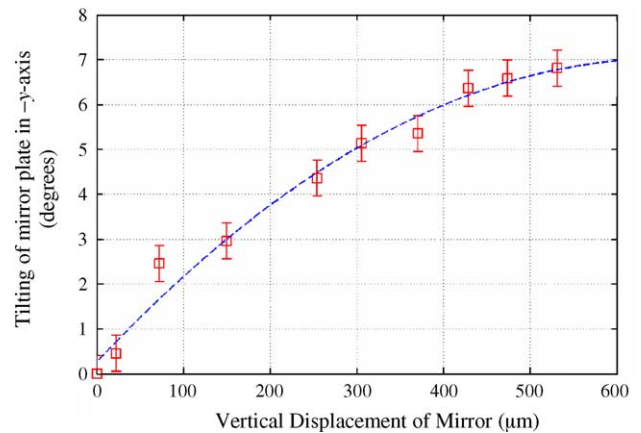

Fig. 12. Tilting of the mirror plate in the negative *y*-direction (due to thermal coupling) as a function of vertical position of the mirror.

mirror; however, the scanned area would be displace towards the −*y*-direction with increasing *z*-displacement (as observed in Fig. 12).

5. Conclusion

An electrothermally actuated 2D micromirror was successfully demonstrated. By using two sets of LVD microactuators the micromirror has the ability to perform bi-directional 2D scans.

Optical scan angles larger than $\pm 30°$ have been obtained in two dimensions with driving voltages less than 12 V. 2D dynamic scanning using this mirror has also been demonstrated by obtaining a $14° \times 50°$ angular raster scan pattern. This device also has the ability to perform vertical displacements of up to 0.5 mm along the z-axis, thereby permitting 2D scanning in the vertical direction. The mirror fabrication process is mask-less, uses only dry etch steps, and is completely compatible with foundry CMOS processes. Since, this fast-scanning micromirror scans large optical angles at low actuation voltages, it is suitable for use in endoscopic biomedical imaging applications.

Acknowledgement

References

[1] P.F.V. Kessel, L.J. Hornbeck, R.E. Meier, M.R. Douglass, A MEMS-based projection display, Proc. IEEE 98 (1998) 1687–1704.

[2] R.A. Conant, P. Hagelin, U. Krishnamoorthy, O. Solgaard, K.Y. Lau, R.S. Muller, A raster-scanning full-motion video display using polysilicon micro machined mirrors, Sens. Actuators A 83 (2000) 291–296.

[3] H. Xie, Y. Pan, G.K. Fedder, Endoscopic optical coherence tomography imaging with a CMOS-MEMS micromirror, Sens. Actuators A 103 (2003) 237–241.

[4] T.W. Yeow, K.Y. Lim, B. Wilson, A.A. Goldenberg, A low-voltage electrostatically actuated MEMS scanner for in vivo bio medical imaging, in: Technical Digest of the 2nd Annual International IEEE-EMB Special Topic Conference on Microtechnologies in Medicine & Biology, Madison, WI, 2002 May, pp. 205–207.

[5] J.M. Zara, J.A. Izatt, K.D. Rao, S. Yazdanfar, S.W. Smith, Scanning mirror for optical coherence tomography using an electrostatic MEMS actuator, in: Technical Digest of the 2002 IEEE International Symposium on Biomedical Imaging, July 2002, pp. 297–300.

[6] D.S. Greywall, P.A. Busch, F. Pardo, D.W. Carr, G. Bogart, H.T. Soh, Crystalline silicon tilting mirrors for optical cross-connect switches, J. Microelectromech. Syst. 12 (2003) 708–712.

[7] J.J. Bernstein, W.P. Taylor, J.D. Brazzle, C.J. Corcoran, G. Kirkos, J.E. Odhner, A. Pareek, M. Waelti, M. Zai, Electromagnetically actuated mirror arrays for use in 3-D optical switching applications, J. Microelectromech. Syst. 13 (2004) 526–535.

[8] A. Baba, H. Okano, H. Uetsuka, M. Esashi, 2 Axes Optical Switch With Holding Mechanism, in: Technical Digest of the 16th IEEE International Conference on Micro Electro Mechanical Systems (MEMS'03), Kyoto, Japan, January 2003, pp. 251–254.

[9] H. Schenk, P. Durr, D. Kunze, H. Lakner, H. Kuck, A resonantly excited 2D-micro-scanning-mirror with large deflection, Sens. Actuators A 89 (2001) 104–111.

[10] I.J. Cho, K.S. Yun, H.K. Lee, J.B. Yoon, E. Yoon, A low-voltage two-axis electromagnetically actuated micromirror with bulk silicon mirror plates and torsion bars, in: Technical Digest of the 15th IEEE International Conference on Micro Electro Mechanical Systems (MEMS'02), Las Vegas, NV, January 2002, pp. 540–543.

[11] N. Kikuchi, Y. Haga, M. Maeda, W. Makishi, M. Esashi, Piezoelectric 2-D micro scanner for minimally invasive therapy fabricated using femtosecond laser ablation, in: Technical Digest of the 12th International Conference on Solid-State Sensors, Actuators and Microsystems (TRANSDUCERS'03), Boston, MA, June 2003, pp. 603–606.

[12] H.-J. Nam, Y.-S. Kim, S.-M. Cho, Y. Yee, J.-U. Bu, Low voltage PZT actuated tilting micromirror with hinge structure, in: Technical Digest of the IEEE/LEOS International Conference on Optical MEMS, Lugano, Switzerland, August 2002, pp. 89–90.

[13] S.J. Kim, Y.H. Cho, H.J. Nam, J.U. Bu, Piezoelectrically pushed rotational micromirrors for wide-angle optical switch applications, in: Technical Digest of the 16th IEEE International Conference on Micro Electro Mechanical Systems (MEMS'03), Kyoto, Japan, January 2003, pp. 263–266.

[14] G.-D. Su, H. Toshiyoshi, M.C. Wu, Surface-micromachined 2-D optical scanners with high-performance single-crystalline silicon micromirrors, IEEE Photonic Technol. Lett. 13 (2001) 606–608.

[15] T. Kudrle, C. Wang, M. Bancu, J. Hsiao, A. Pareek, M. Waelti, G. Kirkos, T. Shone, C. Fung, C. Mastrangelo, Single-crystal silicon micromirror array with polysilicon flexures, Sens. Actuators A 119 (2005) 559–566.

[16] M.R. Dokmeci, A. Pareek, S. Bakshi, M. Waelti, C.D. Fung, K.H. Heng, C.H. Mastrangelo, Two-axis single-crystal silicon micromirror arrays, J. Microelectromech. Syst. 13 (2004) 1017.

[17] S. Kwon, V. Milanovic, L.P. Lee, Vertical combdrive based 2-D gimbaled micromirrors with large static rotation by backside island isolation, IEEE J. Sel. Top. Quant. Electron. 10 (2004) 498–504.

[18] W. Piyawattanametha, P.R. Patterson, D. Hah, H. Toshiyoshi, M.C. Wu, A 2-D scanner by surface and bulk micromachined angular vertical comb actuators, in: Technical Digest of the 2003 IEEE/LEOS International Conference on Optical MEMS, Waikoloa, Hawaii, August 2003, pp. 93–94.

[19] V. Milanovic, G.A. Mathus, D.T. McCormick, Gimbal-less monolithic silicon actuators for tip-tilt-piston micromirror applications, IEEE J. Sel. Top. Quant. Electron. 10 (2004) 462–471.

[20] S. Schweizer, P. Cousseau, G. Lammel, S. Calmes, P. Renaud, Two-dimensional thermally actuated optical microprojector, Sens. Actuators A 85 (2000) 424–429.

[21] A. Jain, A. Kopa, Y. Pan, G.K. Fedder, H. Xie, A Two-Axis Electrothermal Micromirror for Endoscopic Optical Coherence Tomography, IEEE J. Sel. Top. Quant. Electron. 10 (2004) 636–642.

[22] A. Jain, H. Qu, S. Todd, H. Xie, A thermal bimorph micromirror with large bi-directional and vertical actuation, Sens. Actuators A 122 (2005) 9–15.

[23] A. Jain, S. Todd, H. Xie, An electrothermally-actuated, dual-mode micromirror for large bi-directional scanning, in Technical Digest of the 2004 IEEE International Electron Devices Meeting (IEDM 2004), San Francisco, CA, December 2004, pp. 47–50.

[24] H. Xie, L. Erdmann, X. Zhu, K. Gabriel, G.K. Fedder, Post-CMOS processing for high-aspect-ratio integrated silicon micro structures, J. Microelectromech. Syst. 11 (2002) 93–101.

[25] MOSIS integrated circuit fabrication service. Marina del Rey, CA.

[26] S.T. Todd, H. Xie, An analytical electrothermal model of a 1-D electrothermal MEMS micromirror, Proc. SPIE 5649 (2004) 344–353.

Biographies

Ankur Jain received his BE (Honors) degree in electrical and electronics engineering from the Birla Institute of Technology and Science (BITS), Pilani, India in 2000, and his MS degree in electrical engineering from the University of Florida, Gainesville in 2002. He is currently working towards a PhD degree at the Biophotonics and Microsystems Laboratory at the University of Florida, Gainesville. His research interests include the design, fabrication and packaging of CMOS MEMS devices for biomedical imaging, endoscopic optical coherence microscopy, and photonic devices.

Huikai Xie is an assistant professor at the Department of Electrical and Computer Engineering of the University of Florida. He received his MS in electro-optics from Tufts University in 1998, and PhD degree in electrical and computer engineering from Carnegie Mellon University in 2002. He also holds BS and MS degrees in electronic engineering from Beijing Institute of Technology. From 1992 to 1996, he was a faculty member of the Institute of Microelectronics at Tsinghua University, Beijing, working on various silicon-based chemical and mechanical sensors. He has published over 40 technical papers. His present research interests include micro/nanofabrication, integrated microsensors, optical MEMS and optical imaging.